Optics Letters

Optimal operational conditions for supercontinuum-based ultrahigh-resolution endoscopic OCT imaging

Wu Yuan,[1] Jessica Mavadia-Shukla,[1] Jiefeng Xi,[1] Wenxuan Liang,[1] Xiaoyun Yu,[2] Shaoyong Yu,[2] and Xingde Li[1,*]

[1]Department of Biomedical Engineering, School of Medicine, Johns Hopkins University, Baltimore, Maryland 21205, USA
[2]Department of Medicine, School of Medicine, Johns Hopkins University, Baltimore, Maryland 21205, USA
*Corresponding author: xingde@jhu.edu

Received 23 October 2015; revised 7 December 2015; accepted 7 December 2015; posted 8 December 2015 (Doc. ID 252488); published 6 January 2016

We investigated the optimal operational conditions for utilizing a broadband supercontinuum (SC) source in a portable 800 nm spectral-domain (SD) endoscopic OCT system to enable high resolution, high-sensitivity, and high-speed imaging *in vivo*. A SC source with a 3-dB bandwidth of ~246 nm was employed to obtain an axial resolution of ~2.7 μm (in air) and an optimal detection sensitivity of ~ − 107 dB with an imaging speed up to 35 frames/s (at 70 k A-scans/s). The performance of the SC-based SD-OCT endoscopy system was demonstrated by imaging guinea pig esophagus *in vivo*, achieving image quality comparable to that acquired with a broadband home-built Ti:sapphire laser.

OCIS codes: (170.2150) Endoscopic imaging; (110.4500) Optical coherence tomography; (170.3880) Medical and biological imaging; (320.6629) Supercontinuum generation.

http://dx.doi.org/10.1364/OL.41.000250

OCT endoscopy has become a powerful technology enabling a variety of translational applications [1]. This technology affords highresolution "optical biopsies" without the need for tissue removal or processing. It is well known that the axial resolution of the OCT system is quadratically proportional to the central wavelength, and inversely proportional to the spectral bandwidth of the low coherence light source. To achieve high-resolution, a broad spectral bandwidth is thus needed. More effectively, high-resolution can be readily achieved with a low coherence source of a short central wavelength (for a given spectral bandwidth) due to the quadratic dependency. This was well recognized and demonstrated a long time ago [2]. By moving the central wavelength from 1300 to 800 nm, the axial resolution has been greatly improved from 10 μm down to several microns [2]. In addition, the image contrast can be potentially enhanced owing to the increased light scattering and lower tissue absorption around 800 nm, although the penetration depth may become shorter [3–5].

One possible choice of a broadband light source at 800 nm is an ultra-short pulsed Ti:sapphire laser, which can provide a broad bandwidth, high output power, and low intensity noise. Ultrahigh-resolution OCT imaging with a 5 fs Ti:sapphire laser has been previously demonstrated [2]. One considerable challenge with a short-pulsed Ti:sapphire laser is its bulky size, high cost, and the requirement of skilled operation and maintenance. Thus, it is not ideal for translational OCT applications. Another ultra-broadband light source at 800 nm is the super luminescent diode (SLD). By combining several SLDs with different central wavelengths around 800 nm [6], this light source is portable with low intrinsic noise, and can also offer a broad bandwidth. However, the challenge to use such a SLD-based light source for endoscopic applications is its limited output power. A supercontinuum (SC) source, on the other hand, can easily offer a broad and selectable spectrum with ample output power [7]. It is an excellent alternative considering the SC source is becoming more compact and permits turn-key operation. The great potential of a SC source has been demonstrated in several 800 nm bench-top systems with the best reported axial resolution of ~3 μm in air [8,9].

However, a SC source has its own challenges, and the major challenge is its noise is often much higher than a Ti:sapphire laser or a SLD, since most commercially available SC sources operate in the modulation instability region in order to achieve a broad spectrum, as well as, scalability to a high output power [10]. In order to fully utilize the broad bandwidth and the high power of a SC source to achieve high-resolution and good signal-to-noise ratio in a portable endoscopic OCT system, it is critical to manage the noise properties of a SC-based OCT system.

In this Letter, we investigated and identified the optimal operational conditions for utilizing a compact broadband SC source around 800 nm to enable high-resolution, high-sensitivity, and high-speed *in vivo* imaging in a portable endoscopic spectral-domain (SD) OCT system. *In vivo* 3D circumferential endoscopic imaging was performed on guinea pig esophagus with the SC-based endoscopic OCT system under the optimal operational

conditions. It was found that the image's quality achieved with such a system is very much comparable with that acquired with a home-built 7 fs Ti:sapphire laser.

A customized SC source (SuperK extreme low noise) from NKT Photonics with a repetition rate of ~325 MHz was employed in this study. An external spectrum shaping setup (Fig. 1A) consisting of a prism pair and a spatial filter was employed to achieve a broad bandwidth and a good spectral shape. The spectral bandwidth increased with the increase in the SC pump level until the pump level reached about 30% of the maximum pump power. As illustrated in Fig. 1B, a decent spectral shape with a 3 dB spectral bandwidth of ~246 nm and a central wavelength around 800 nm can be achieved. In comparison, the home-built Ti:sapphire laser has a 3 dB bandwidth of ~150 nm with a central wavelength around 830 nm (also shown in Fig. 1B).

After achieving a good spectrum (e.g., of a broad bandwidth and a near Gaussian spectral profile at a central wavelength of around 800 nm), we studied the noise characteristics of the SC source. The SC power spectrum was measured with a fast Si photodiode and an electronic spectrum analyzer (ESA). As shown in Fig. 1C, a pronounced noise floor (red line, fitted from the measured power spectrum with the laser pulse and harmonic peaks removed) was observed for the SC source. For comparison, the noise floor of the home-built Ti:sapphire laser (black line) measured with the same experimental and ESA settings is also illustrated in Fig. 1C. By using the mean noise floor value at frequencies from 0 to 70 kHz [the maximum A-lines sampling rate of the line charge-coupled device (CCD) in our SD-OCT system], we find the laser excess noise of the SuperK versus pump power level, as shown in Fig. 1D. It can be seen that the noise increased gradually and reached a plateau at about 30% of the maximum pump power level, where the spectrum of the SC source also became stabilized.

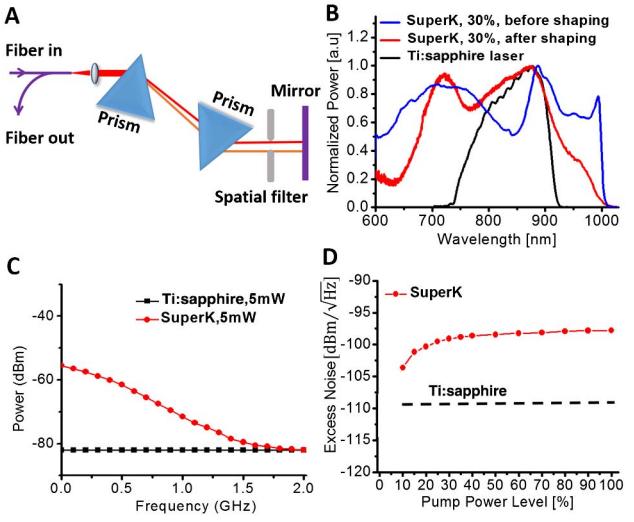

Fig. 1. A, schematic of the spectrum shaping setup; B, spectra of SuperK before shaping (blue curve) and after shaping (red curve) at 30% pump power level. The black curve shows the spectrum of our home-built Ti:sapphire laser for comparison; C, noise floors of the SuperK (red line) and Ti:sapphire laser (black line) at 5 mW; D, laser excess noise of the SuperK under different pump levels (red dotted line) and the Ti:sapphire laser (black dashed line) averaged over the frequency range of 0–70 kHz.

For all our endoscopic operations, we chose the 30% pump power level in order to leverage the good operational spectrum and sufficient output power from the SuperK. It is noted that the noise of the SuperK at the 30% pump power level was about 12 dBm/$\sqrt{\text{Hz}}$ higher than the noise (black dash line in Fig. 1D) of the Ti:sapphire laser.

It is well known that the OCT system should be operated under the shot-noise limited conditions in order to achieve optimal imaging performance. To find out the conditions under which the SC-based OCT system can be operated in the shot-noise limited region, an SC-based SD-OCT endoscopy system was employed. As shown in Fig. 2A, this endoscopic OCT system adopted a customized broadband linear-in-wavenumber spectrometer, the details of which were reported previously [5]. In essence, this spectrometer can accommodate a spectrum bandwidth of ~250 nm around an 800 nm central wavelength and offer an imaging depth of ~1.2 mm. A 1200 lines/mm grating was used in the spectrometer. A prism was inserted after the grating to achieve a linear wavenumber distribution over the broad spectrum. A custom designed multi-element scan lens was used to focus the linearly dispersed light onto a line scan CCD camera. The line CCD has 2048 pixels and an

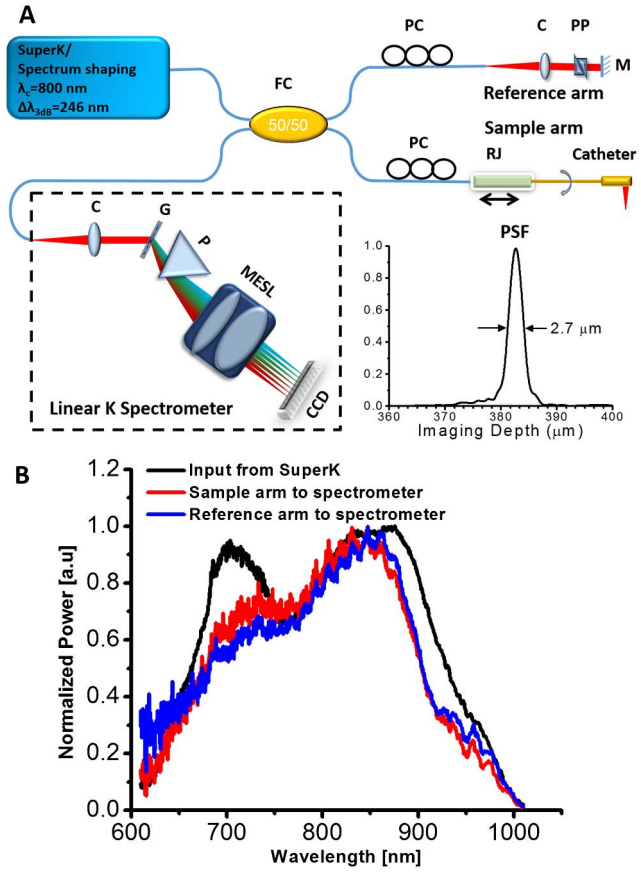

Fig. 2. A, schematic of the ultrahigh-resolution endoscopic SD-OCT system and the measured point spread function (PSF, inset). C, multi-element achromatic collimator; G, grating; FC, fiber coupler; M, mirror; MESL, multi-element scan lens; P, linear K mapping prism; PC, polarization controller; PP, prism pair; RJ, fiber-optic rotary joint. B, spectrum of the SuperK input to the SD-OCT system (black line) and the back-reflected spectra by a mirror from the sample arm (red line) and reference arm (blue line) to the spectrometer.

A-scan rate of up to 70 kHz (i.e., 70 k A-scans/s) at a 12 bit resolution. The measured roll-off performance of the spectrometer is ~ – 13.3 dB/mm.

In the endoscope, a diffractive lens was introduced in the distal end to minimize the chromatic aberration over the broad spectrum. The basic distal end optics design was similar to the one reported in reference [5]. The endoscope (including a protective plastic sheath) had an outer diameter of 1.72 mm and a focused spot size of ~4.7 μm at a working distance of ~1.03 mm (from the center of the endoscope). To achieve 3D circumferential scanning, a glass capillary-based rotary joint similar to the one reported in [11] was employed. The rotary unit was mounted on a translational stage to enable pullback during circumferential beam scanning for a performing 3D imaging. This home-made rotary joint was optimized to have a one-way throughput >91%, a back-reflection < – 48 dB, and an optical coupling variation < ± 5% during continuous rotation at a speed up to 35 revolutions/s.

The dispersion between the sample and reference arms was carefully matched by a prism pair made of SF11 flint glass in the reference arm in order to achieve optimal axial resolution. The flint glass provides a much higher group velocity and third-order dispersion than crown glass (e.g., BK7) and optical fiber around 800 nm, and therefore, more effectively minimizes the dispersion mismatch between the two arms. To further optimize the axial resolution, two sets of polarization controllers were used in sample and reference arms, respectively, to manage the polarization mode dispersion. With the SC source at 30% pump level, an axial resolution of ~2.7 μm (in air) was achieved (as shown in the inset of Fig. 2A). This was slightly worse than what was afforded by the SC source due to the suboptimal spectrum throughput bandwidth of the fiber coupler and the collimators in the OCT system. As shown in Fig. 2B, the bandwidths of spectra from the sample and reference arms after passing through the fiber coupler were narrower than that of the input spectrum from the SuperK. In comparison, a resolution of ~3 μm (in air) can be achieved by using the home-built Ti:sapphire laser [5].

To investigate the shot-noise limited condition, we measured the OCT interference signal at different reference arm power levels (quantified with the CCD counts) by gradually increasing the reference arm power with a tunable neutral density (ND) filter. The noise was calculated as the standard deviation from the measured OCT signal. Noise versus the reference arm power level is shown in Figs. 3A and 3B for the OCT system with the SuperK and the Ti:sapphire laser, respectively. Linear fitting was performed on the noise measurements versus reference arm power with a target R^2 value (coefficient of determination) of 0.95 in order to identify the shot-noise limited region. The fitted blue line with a slope of ½ in Fig. 3A shows that with the SuperK source there was a narrow reference arm power region (i.e., between ~100 and ~1000 CCD counts) in the middle portion of the noise curve, where the noise followed the square root dependency on the reference arm power level, signifying the shot-noise limited operation region. Beyond this region at the upper portion of the noise curve, the laser excess noise dominating region can be identified with a linearly fitted black dash line ($R^2 = 0.95$) of a slope of 1 in the log-log plot. For the best operation with the SC source, we make sure the reference arm power level is carefully chosen to fall within the shot-noise limited region. In order to have a high OCT homodyne

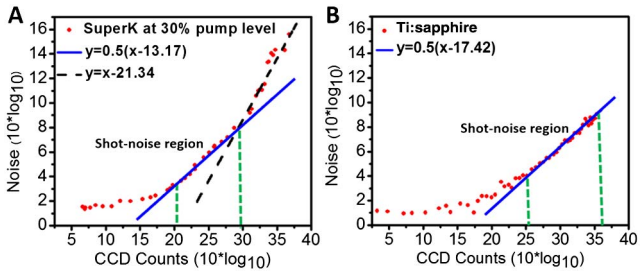

Fig. 3. Noise versus reference arm power level for an SD-OCT system, with A, the SuperK and B, the Ti:sapphire laser as the light source. The blue lines in A and B represent linear fitting for the shot-noise limited reference arm power region. Black dashed line in A represents linear fitting for the laser excess noise dominating region.

gain and a low noise floor, we chose to operate the SC-based OCT system at the upper portion of the shot-noise limited region, corresponding to ~1000 CCD counts. In contrast, with the Ti:sapphire laser a much broader shot-noise limited region can be achieved (i.e., between ~315 and 4096 CCD counts), as shown in Fig. 3B.

Under the optimal operational conditions, i.e., at the 30% SC pump level with a good source spectrum and an ~6.1 μW optical power from the reference arm (corresponding to ~1000 CCD counts), the measured detection sensitivity with an incident power of ~9 mW in the sample arm was about –107 dB at a 70 kHz A-scans/s, which is very close to the detection sensitivity (~ – 108 dB) when using a Ti:sapphire laser with the same optical power in the sample arm. It is noteworthy that the detection sensitivity was measured with the widely used method, the detail of which was reported previously [8]. When increasing the reference arm power from ~6.1 μW (~1000 CCD counts) to ~13 μW (~2500 CCD counts), the SC-based endoscopic SD-OCT system operated in a suboptimal condition (i.e., laser excess noise dominating region). Under this suboptimal condition and with the same power in the sample arm (~9 mW), the measured detection sensitivity decreased to approximately –103 dB.

The performance of the ultrahigh-resolution SC-based SD-OCT endoscopy system under the optimal operational conditions (e.g., with a reference arm power of ~6.1 μW) was tested for 3D imaging of a guinea pig esophagus *in vivo* under an imaging protocol approved by the Animal Care and Use Committee at Johns Hopkins University. With 2 k to 8 k A-scans/frame, an imaging speed up to 35 frames/s was achieved. A representative 2D circumferential image is shown in Fig. 4A. Figure 4B shows a cutaway view of a 3D image reconstructed from a series of 2D images acquired along the longitudinal axis of the esophagus with a 10 μm pitch. As shown in Fig. 4C which is the 2X zoomed-in image over the boxed region in Fig. 4A, all layered structures of the guinea pig esophagus, such as the stratum corneum, epithelium, lamina propria, submucosa, and muscularis propria, can be clearly identified. Fine structures, such as the thin layer of muscularis mucosae that is embedded between lamina propria and submucosa, can also be easily identified. The corresponding histology is shown in Fig. 4D, and the excellent correlation between OCT image and histology is evident.

In vivo imaging was also conducted with the same system but under a suboptimal condition (e.g., with a reference arm

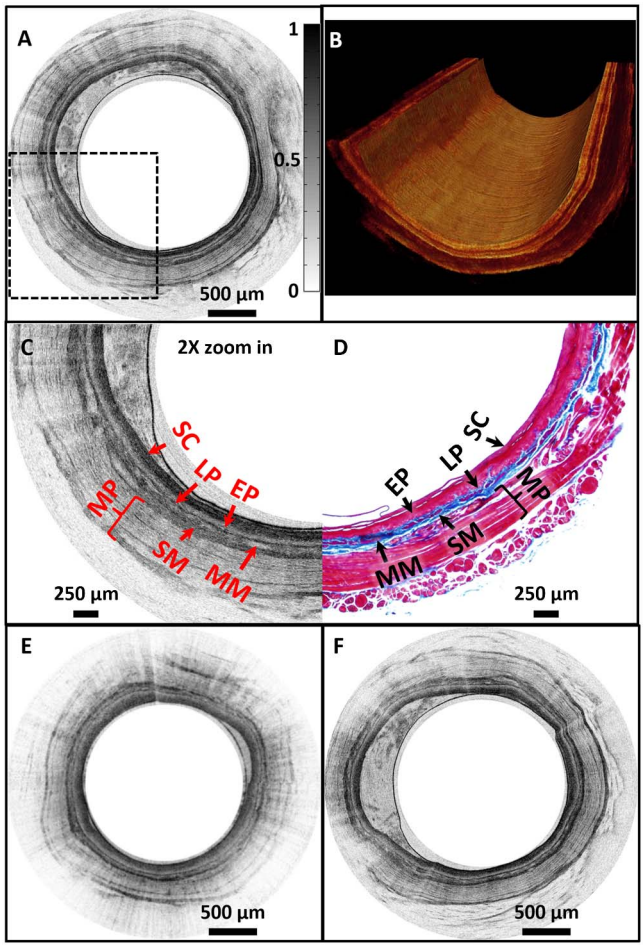

Fig. 4. A, representative *in vivo* 2D OCT image; B, 3D cutaway view of a guinea pig esophagus acquired with a SuperK source under optimal operational conditions; C, 2X zoomed-in view of the boxed region in A; D, corresponding histology; E, representative *in vivo* 2D OCT image acquired with a SuperK source under suboptimal operational condition; F, representative *in vivo* 2D OCT image acquired with a Ti:sapphire laser-based SD-OCT system under shot-noise limited condition. All images were acquired with the imaging speed of ~4.9 frames/s and processed with the same gray scale. SC, stratum corneum; EP, epithelium; LP, lamina propria; MM, muscularis mucosae; SM, submucosa; MP, muscularis propria.

power of ~13 μW), and a representative image is shown in Fig. 4E. In addition, a representative image acquired with similar experimental conditions but with the home-built Ti:sapphire laser (i.e., with the reference arm power of ~13 μW or ~2500 CCD counts which was within the shot-noise limited region of the Ti:sapphire laser-based SD-OCT system) is shown in Fig. 4F. It can be found that the image quality acquired by the SuperK-based SD-OCT endoscopy system under the optimal operational condition (Fig. 4A) is better than that acquired under the suboptimal condition (Fig. 4E), and is very similar with the one acquired with the Ti:sapphire laser-based SD-OCT system (Fig. 4F).

In summary, we investigated the optimal operational conditions for an 800 nm endoscopic SD-OCT system that utilized a broadband SC source to enable ultrahigh-resolution, high-sensitivity, and high-speed endoscopic OCT imaging. The use of an SC source makes the OCT system compact, portable, and enables turn-key operation. Combined with a home-built high-resolution endoscope and a fiber-optic rotary joint, real-time 3D OCT imaging of a guinea pig esophagus was demonstrated *in vivo*. The animal experiments demonstrated that the imaging quality with an SC-based OCT system under optimal operational conditions is similar to that acquired with a 7 fs Ti:sapphire laser-based SD-OCT system.

Funding. National Institutes of Health (NIH) (R01CA153023, R01HL121788).

Acknowledgment. The authors would also like to acknowledge their useful discussions with Dr. Husain Imam and Dr. Thomas Feuchter from NKT Photonics.

REFERENCES

1. G. J. Tearney, M. E. Brezinski, B. E. Bouma, S. A. Boppart, C. Pitris, J. F. Southern, and J. G. Fujimoto, Science **276**, 2037 (1997).
2. B. Bouma, G. J. Tearney, S. A. Boppart, M. R. Hee, M. E. Brezinski, and J. G. Fujimoto, Opt. Lett. **20**, 1486 (1995).
3. A. R. Tumlinson, B. Povazay, L. P. Hariri, J. McNally, A. Unterhuber, B. Hermann, H. Sattmann, W. Drexler, and J. K. Barton, J. Biomed. Opt. **11**, 064003 (2006).
4. D. Wang, B. V. Hunter, M. J. Cobb, and X. D. Li, IEEE J. Sel. Top. Quantum Electron. **13**, 1596 (2007).
5. J. F. Xi, A. Zhang, Z. Liu, W. X. Liang, L. Y. Lin, S. Yu, and X. D. Li, Opt. Lett. **39**, 2016 (2014).
6. T. H. Ko, D. C. Adler, J. G. Fujimoto, D. Mamedov, V. Prokhorov, V. Shidlovski, and S. Yakubovich, Opt. Express **12**, 2112 (2004).
7. I. Hartl, X. D. Li, C. Chudoba, R. K. Ghanta, T. H. Ko, J. G. Fujimoto, J. K. Ranka, and R. S. Windeler, Opt. Lett. **26**, 608 (2001).
8. P. Cimalla, J. Walther, M. Mehner, M. Cuevas, and E. Koch, Opt. Express **17**, 19486 (2009).
9. Z. Zhi, J. Qin, L. An, and R. K. Wang, Opt. Lett. **36**, 3169 (2011).
10. W. Yuan, Laser Phys. Lett. **10**, 095107 (2013).
11. X. D. Li, C. Chudoba, T. Ko, C. Pitris, and J. G. Fujimoto, Opt. Lett. **25**, 1520 (2000).